Pergamon

Cement and Concrete Research, Vol. 28, No. 3, pp. 349–355, 1998

0008-8846/98 $19.00 + .00

PII S0008-8846(97)00276-7

EFFECT OF AGING ON THE FRACTURE CHARACTERISTICS AND BRITTLENESS OF A HIGH-STRENGTH CONCRETE

R. Gettu,[1] V.O. Garcia-Álvarez, and A. Aguado
Universitat Politècnica de Catalunya, ETSECCPB, Gran Capitán, s/n,
E-08034 Barcelona, Spain

(Received November 25, 1997; in final form December 19, 1997)

ABSTRACT

Results of notched beam (fracture) tests on a 60-MPa silica fume concrete at the ages of 4, 10, 31, and 232 days are presented. Fracture parameters at the different ages were obtained using the size effect and cohesive crack models, which indicate that the fracture resistance (toughness and energy) decreases and the brittleness increases with the age of the concrete. This trend is attributed to the increase in the strength of the hardened cement paste and the interfaces that leads to less bond cracking and more aggregate rupture, and, consequently, to more brittle failure and lower toughening. *© 1998 Elsevier Science Ltd*

Introduction

The failure of high-strength silica fume concrete is characteristically more brittle than that of conventional concretes. This can be attributed to the compact high-strength matrix and interfaces, which reduce the toughening that can occur during crack propagation (1,2), although increasing the strength and impermeability of the concrete. This phenomenon can be studied using models based on fracture mechanics that are capable of quantifying the effectiveness of the toughening mechanisms, as well as the crack resistance, through material parameters.

In the present work, the evolution of the fracture parameters with age (ranging from 4 days to 8 months) is studied using two different models. One of them is an effective crack model, known as the size effect model, through which fracture parameters can be derived from the peak loads of notched specimens of different sizes (3,4). Here the model is applied to data from beams undergoing mode I fracture. The second is a cohesive crack model, defined through a constitutive relation for the stress vs. crack separation response (5), which in the present work is implemented in a finite element framework using joint elements and a discrete crack approach. Experimentally obtained load vs. crack mouth opening displacement (CMOD) curves of notched beams have been used to determine the parameters of the latter model.

Communicated by Z.P. Bazant.
[1]To whom correspondence should be addressed.

TABLE 1
Concrete properties.

Batch	28-day cylinder compressive strength (MPa)	Slump (cm)
A	64.3 (±6.9%)	23
B	67.5 (±5.3%)	24
C	60.6 (±1.5%)	22
D	68.1 (±6.6%)	20

Details of the Material, Specimens, and Tests

The concrete used in this study was designed for a 28-day compression strength of 60 MPa, with the proportions of cement:sand:gravel:microsilica:water as 1:1.25:1.8:0.2:0.3. Spanish type I/55A cement (equivalent to European Standard CEM I 52.5R cement), densified silica fume, crushed basalt gravel (5–12 mm), and siliceous sand (0–5 mm) were used. A melamine-based superplasticizer was also incorporated in the concrete. Four batches of the concrete were fabricated for the experimental study. The slump of each of them is given in Table 1. Three 150 mm × 300 mm cylinders and nine beams were cast from each batch. The ends of the cylinders were polished with a diamond wheel and they were tested in compression 28 days after casting; the average strengths (f_c) are reported in Table 1. The beams had the same thickness (b) of 50 mm, depths (d) of 80, 160, and 320 mm, lengths equal to 3.125d, and spans equal to 2.5d. Three beams were cast for each d. A notch of length $a_0 = 0.275d$ was cut at the mid-span of each beam with a diamond disc saw. All specimens were stored in a fog room until testing.

The tests of the notched beams were conducted in a 1 MN INSTRON servohydraulic machine under closed-loop CMOD control. Constant CMOD rates were imposed, such that the peak loads occurred at about 3 min. Each batch of beams was tested at a different age (see Table 2) and the load-CMOD curves of the specimens were recorded. Visual observations of the crack surfaces showed, as expected, a significant increase in the number of ruptured gravel aggregates with an increase in age; for example, it doubled between the ages of 4 days and 8 months in the largest beams. The peak loads obtained in the tests are given in Table 2 (except for one 160 mm specimen of series C that was not registered). In general, there is no major increase in the failure loads with age, especially in the larger specimens.

TABLE 2
Peak loads of the notched beams at different ages.

		Peak loads of individual specimens, P_u (N)		
Batch	Age (days)	d = 80 mm	d = 160 mm	d = 320 mm
A	4	3925, 4125, 3500	6424, 6408, 6400	12370, 12650, 12650
B	10	3888, 3950, 3950	7175, 7150, 7725	12150, 12100, 13300
C	31	4250, 3910, 4738	6900, 8025	12250, 12600, 11700
D	232	4782, 4750, 5100	7450, 8125, 7441	12190, 12640, 12620

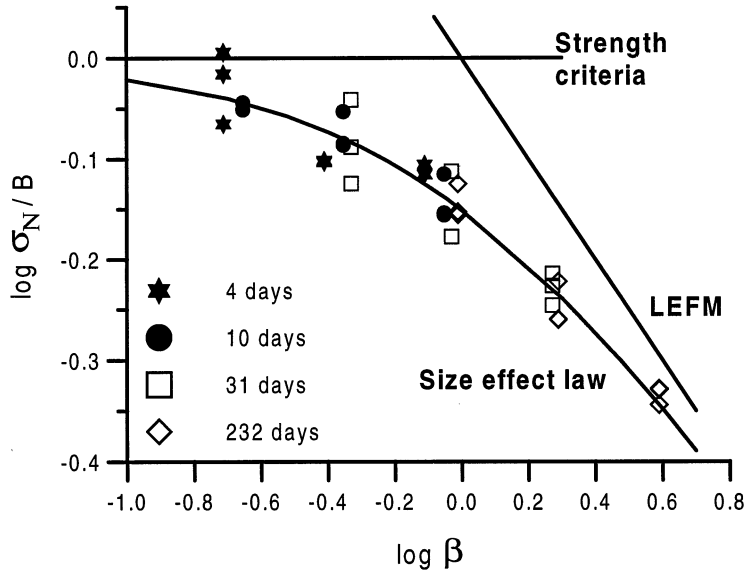

FIG. 1.
Size effect model with normalized experimental data for different ages.

Application of the Size Effect Model

The size effect model (SEM) of Bažant is based on the ductile-brittle transition of the failure mode of geometrically-similar fracture specimens with an increase in size. The basic form of this nonlinear fracture mechanics model, which gives the size-dependence of the nominal failure stress, is (3):

$$\sigma_N = \frac{B}{\sqrt{1+\beta}}; \quad \beta = \frac{d}{d_0} \tag{1}$$

where $\sigma_N = P_u/bd$ is the maximum nominal stress, P_u is the maximum load, d is a characteristic dimension of the specimen (note that here d is the beam depth), and B and d_0 are empirical parameters. β is called the brittleness number and denotes the proximity of the failure mode to ideal-brittle linear elastic fracture mechanics (LEFM) behavior; σ_N has a constant value at $\beta \rightarrow 0$ and is proportional to $d^{-1/2}$ (which corresponds to the LEFM failure criterion) at $\beta \rightarrow \infty$ (Fig. 1). Parameters B and d_0 are obtained by fitting Eq. 1 to the σ_N values determined experimentally from different sizes of specimens.

The values of B and d_0 can be used to obtain material fracture parameters defined unambiguously by Bažant in terms of an infinite size specimen, whose behavior is theoretically independent of geometry effects (3):

$$K_{Ic} = \frac{B}{\sqrt{d_0\, g(\alpha_0)}}; \quad c_f = d_0 \frac{g(\alpha_0)}{g'(\alpha_0)}; \quad G_f = \frac{K_{Ic}^2}{E} \tag{2}$$

where K_{Ic} = fracture toughness, c_f = effective fracture process zone length, G_f = fracture energy, E = modulus of elasticity (for plane stress), and $\alpha_0 = a_0/d$ is the relative notch

TABLE 3
Fracture parameters obtained with the size effect model at different ages.

Age (days)	B (MPa)	d_0 (mm)	ω	E (GPa)	K_{Ic} (MPa-mm$^{1/2}$)	c_f (mm)	G_f (J/m^2)
4	1.02	413	0.08	32.7	67.5	92	139.3
10	1.10	361	0.04	35.5	67.9	80	129.5
31	1.30	172	0.08	36.8	55.6	38	84.1
232	1.70	82	0.04	38.3	50.3	18	66.0

length. Function g is the dimensionless energy release rate and g' is its derivative with respect to the relative crack length. These functions depend only on the specimen geometry, and can be obtained from LEFM analysis (see Ref. 4 for beam geometries).

The SEM parameters were obtained by regression analysis of σ_N values (from the P_u-data in Table 2 corrected for self-weight, as in Ref. 4), at different ages with Eq. 1, using the Marquardt-Levenberg least-squares algorithm. The normalized experimental data are shown in Fig. 1, where a shift of the data toward the LEFM asymptote, indicating increasing brittleness, is seen with an increase in age. The parameters are given in Table 3, along with the coefficient of variation of the fits (ω). It can be seen that B increases with age while d_0 decreases. Considering that the parameter B is a measure of the strength, the trend observed is logical. The decrease in d_0 indicates an increase in the structural brittleness β.

The modulus of elasticity (E) of each specimen was computed from its initial load-CMOD compliance using LEFM functions; the average value at each age is given in Table 3. As expected, there is an increase in E with age. The values $g(\alpha_0) = 10.6$ and $g'(\alpha_0) = 47.7$ (for $\alpha_0 = 0.275$), obtained by finite element analysis (6), were used in Eq. 2 to determine the material fracture parameters at different ages (given in Table 3). All of them exhibit a decreasing trend with age; the trends of K_{Ic} and G_f indicate a decrease in the toughening and crack resistance, and the decrease in c_f indicates an increase in the brittleness of the material with age (1,7).

Application of the Cohesive Crack Model

The toughening or crack-shielding effect of the fracture process zone that occurs in front of a progressing crack (2) is modeled as closing stresses in cohesive crack models (see Fig. 2). One such model is the fictitious crack model, proposed for concrete by Hillerborg et al. (5). The constitutive relation for the cohesive crack is given by a stress vs. crack separation curve, $\sigma = f(\omega)$. In the present work, the exponential curve shown in Figure 3, which is characterized by two independent parameters, namely the fracture energy (the area under the curve) G_F and the tensile strength f_t, is used. This model has been implemented in a finite element code with the cracking simulated by quadratic joint elements. Further details of the numerical analysis are available in Ref. 6.

The parameters of the cohesive crack for each age were obtained by back-fitting of the experimental load-CMOD curves of all the specimens at that age. Note that all the sizes were fitted together in order to reduce the uncertainty of the parameter set. However, the choice of the optimum parameters was influenced by the trends seen in the size effect analysis, and they are, therefore, not considered to be completely unique or objective. The parameter set,

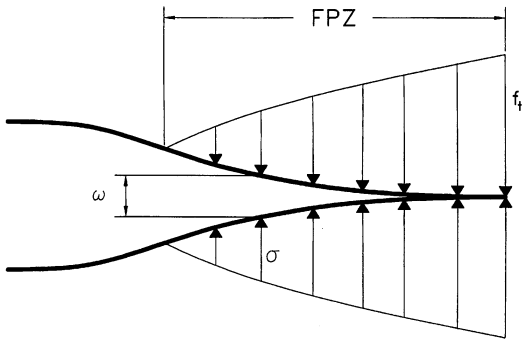

FIG. 2.
Cohesive crack model, where FPZ = fracture process zone.

G_F and f_t, which gave the best fits of the experimental load-CMOD data for the three sizes, are given in Table 4 for each age.

It can be seen that an increase in the tensile strength with age is accompanied by a decrease in G_F, which is similar to the trend of G_f in the SEM, though the absolute values of G_F are higher, as also seen by other researchers (8). The characteristic length (which is related to the process zone length), defined by Hillerborg (5,9) as $l_{ch} = EG_F/f_t^2$, also decreases with age (Table 4), indicating an increase in brittleness.

Discussion

The trends observed in the size effect analysis suggest that the brittleness of a structure composed of the concrete used in this study would increase with age. This is implied by the shift in the data in Figure 1 to the right (toward ideal-brittle LEFM behavior) and the decrease in c_f with age. The parameter c_f is a measure of the size of the zone where energy is dissipated during crack propagation. This conceptual fracture process zone includes the effects of toughening mechanisms such as crack-deflection, bridging and microcracking. Therefore, a decrease in c_f, as in the present results, implies an increase in the brittleness of the material.

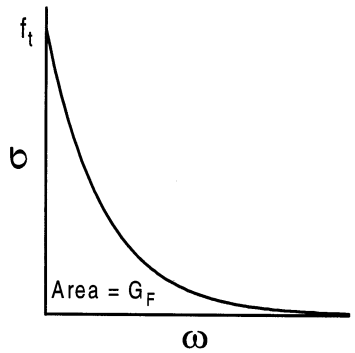

FIG. 3.
Exponential stress vs. crack separation law used in the cohesive crack model.

TABLE 4
Parameters of the cohesive crack model at different ages.

	Age (days)			
Parameter	4	10	31	232
G_F (J/m^2)	150	140	120	88
f_t (MPa)	4.7	5.2	6.0	7.0
l_{ch} (mm)	220	180	120	70

The lower values of K_{Ic} and G_f indicate a slight decrease in the crack resistance, due to the reduced toughening or crack-shielding. A similar trend is seen in the cohesive crack analysis, where an increase in tensile strength with age is accompanied by a decrease in the fracture energy G_F and characteristic length l_{ch}.

The main reason for the increase in brittleness and the decrease in toughening with age seems to be the strengthening of the hardened cement paste and the aggregate-matrix interface due to hardening processes. Moreover, as shown by Alexander (10), the fracture energy of the hardened cement paste decreases with age, implying an increase in its brittleness. Consequently, in high-strength concretes with high matrix and interface strengths, there would be an increase in aggregate rupture and a decrease in interface cracking with age, as observed here in the crack surfaces. The resulting decrease in crack tortuosity would effectively cause a higher stress intensity at the crack-tip or lower toughening, leading to more brittle crack propagation.

In conventional concretes, the failure mechanisms can be significantly different from that of high-strength concretes. At early ages, it has been observed that fracture toughness and fracture energy increase significantly with age (11–13). However, the trends given in the literature for brittleness are contradictory; Petersson (11), and Berra and Castellani (14) found that l_{ch} decreased with age (as in the present results), while Zollinger et al. (13) concluded that c_f increases due to aging. The reasons for the different tendencies seen in the higher strength concretes could be due to the relative strength, toughness, and brittleness of the aggregate, interfaces, and paste, which are obviously influenced by the presence of silica fume and the low water/cement ratio.

Conclusions

High-strength concrete notched beams of three different sizes were tested at the ages of 4, 10, 31 and 232 days. The results were analyzed using the size effect model and the cohesive crack model (with an exponential constitutive law) to obtain the fracture parameters at different ages. The data indicate that the crack resistance decreases and the brittleness increases with age. This can be attributed to the progressive increase in strength and brittleness of the paste, and the strengthening of the interfaces, which lead to more aggregate rupture and less crack tortuosity, causing a decrease in the toughening or crack-shielding.

Acknowledgments

Partial financial support from Spanish CICYT grants PB93-0955 and MAT96-0967, and the Generalitat de Catalunya (DGR-CUR) grant 1995SGR-517 is gratefully appreciated. The doctoral studies of V.O. García-Álvarez at the UPC were supported by a pre-doctoral fellowship from the Generalitat de Catalunya (Spain). The authors thank I. Carol and P.C. Prat for the use of the DRAC finite element package in the numerical analysis, and O.M. García-Álvarez for his help during the tests.

References

1. R. Gettu, Z.P. Bažant and M.E. Karr, ACI Mater. J. 87, 608–618 (1990).
2. R. Gettu and S.P. Shah, High Performance Concrete and Applications, pp. 161–212, Edward Arnold, London, 1994.
3. Z.P. Bažant and M.T. Kazemi, Int. J. Fract. 44, 111–131 (1990).
4. RILEM Technical Committee TC89-FMT, Mater. Struct. 23, 461–465 (1990).
5. A. Hillerborg, M. Modéer, and P.-E. Petersson, Cem. Concr. Res. 6, 773–782 (1976).
6. V.O.García-Álvarez, Study of Mixed Mode Fracture in Quasi-brittle Materials (in Spanish), Doctoral thesis, Universitat Politècnica de Catalunya, Barcelona, Spain, 1997.
7. R. Gettu, P.C. Prat, and M.T. Kazemi, Fracture Mechanics of Concrete Structures, Proceedings FRAMCOS-1, pp. 430–436, Elsevier Applied Science, London, 1992.
8. M. Elices and J. Planas, Adv. Cem. Bas. Mater. 4, 116–127 (1996).
9. A. Hillerborg, Fracture Mechanics of Concrete, pp. 223–249, Elsevier Science, Amsterdam, 1983.
10. M.G. Alexander, Cem. Concr. Res. 24, 1277–1285 (1994).
11. P.E. Petersson, Cem. Concr. Res. 10, 91–101 (1980).
12. F.H. Wittmann, P.E. Roelfstra, H. Mihashi, Y.-Y. Huang, X.-H. Zhang, and N. Nomura, Mater. Struct. 20, 103–110 (1987).
13. D.G. Zollinger, T. Tang, and R.H. Yoo, ACI Mater. J. 90, 463–471 (1993).
14. M. Berra and A. Castellani, Fracture Mechanics of Concrete Structures, Proceedings FRAMCOS-2, pp. 85–94, Aedificatio Publishers, Freiburg, Germany, 1995.